PHOTONICS Research

Robust cavity soliton formation with hybrid dispersion

Jing Wang,[1,2] Yuhao Guo,[1,2] Henan Liu,[1,2] Lionel C. Kimerling,[3] Jurgen Michel,[3] Anuradha M. Agarwal,[3] Guifang Li,[1,2,4] and Lin Zhang[1,2,*]

[1]Key Laboratory of Opto-Electronic Information Technology of Ministry of Education, School of Precision Instrument and Opto-Electronics Engineering, Tianjin University, Tianjin 300072, China
[2]Key Laboratory of Integrated Opto-Electronic Technologies and Devices in Tianjin, School of Precision Instrument and Opto-Electronics Engineering, Tianjin University, Tianjin 300072, China
[3]Department of Materials Science and Engineering, Massachusetts Institute of Technology, Cambridge, Massachusetts 02139, USA
[4]College of Optics and Photonics, CREOL and FPCE, University of Central Florida, Orlando, Florida 32816, USA
*Corresponding author: lin_zhang@tju.edu.cn

Received 22 January 2018; revised 2 April 2018; accepted 3 April 2018; posted 18 April 2018 (Doc. ID 320234); published 24 May 2018

Microresonator-based Kerr frequency combs have attracted a great deal of attention in recent years, in which mode locking of the generated combs is associated with bright or dark cavity soliton formation. In this paper, we show that, different from soliton propagation along a waveguide, cavity solitons can be robustly formed under a unique dispersion profile with four zero-dispersion wavelengths. More importantly, such a dispersion profile exhibits much smaller overall dispersion, thus making it possible to greatly reduce the pump power by five to six times.

OCIS codes: (190.4380) Nonlinear optics, four-wave mixing; (190.3270) Kerr effect.

https://doi.org/10.1364/PRJ.6.000647

1. INTRODUCTION

Pioneering experiments in microcavity-based frequency combs, called Kerr combs, exhibit the possibility of achieving an on-chip comb generator [1–3]. This is of great interest in both scientific research and technological applications. After initial reports, optimizing comb performance becomes increasingly important, aiming at increased comb bandwidth, improved spectral flatness and coherence, and reduced pump power requirement.

As cascaded parametric processes, Kerr combs are generated with careful dispersion engineering. It has been studied in either anomalous or normal dispersion regime [4–11], related with bright or dark solitons. In analogue to a soliton formed in a waveguide or fiber [12], higher-order dispersion's influence on soliton formation has been studied recently [13–18]. Particularly, third-order dispersion may help stabilize cavity solitons. Cavity solitons exhibit unique robustness as a result of pulse reshaping induced by the intra-cavity interference between the soliton and incoming pump. It is recently found that Kerr combs can be generated with a spectrally localized loss [19]. It would be of interest to explore comb generation with a hybrid dispersion, e.g., a dispersion profile with multiple (>2) zero-dispersion wavelengths (ZDWs) [20,21]. A soliton covers a frequency band with anomalous and normal dispersions at different locations. This is known to break stable soliton propagation in a waveguide or fiber [12], but it remains unexplored in the cavity case.

On the other hand, to increase comb bandwidth, it is needed to use a high pump power at the order of watts [22,23]. This contributes to the power consumption of a comb generator, hindering the implementation of a fully integrated Kerr comb using an on-chip pump laser. It is desired to greatly reduce the pump power requirement for broadband Kerr combs.

In this paper, we explore cavity soliton formation with a dispersion profile with four ZDWs and show that, different from soliton propagation along a waveguide, a cavity soliton can be stably supported. Moreover, the pump power required to achieve the same comb bandwidth can be reduced by five to six times by employing hybrid dispersion. We also provide general guidelines for pump power reduction in Kerr comb generation.

2. RESULTS AND DISCUSSION

In the Kerr combs mode locked via cavity soliton formation, if one assumes no higher-order dispersion or other nonlinear effects such as self-steepening or Raman scattering, the comb bandwidth is found proportional to

$$\Delta f_{3\,\mathrm{dB}} \propto \sqrt{\frac{\gamma P_{\mathrm{in}} F}{|\beta_2|}}, \tag{1}$$

where γ is the nonlinear coefficient, F is the finesse of the cavity, and β_2 is the second-order dispersion [24]. For the same comb bandwidth, pump power P_{in} can be reduced if β_2 value is small. However, considering all-order dispersion, β_2 is a function of frequency, and thus we need to make the dispersion low over a wide band to achieve a large comb bandwidth [6] and pump power reduction. Since β_2 is frequency dependent, we need only the overall dispersion experienced by the whole comb to be small and anomalous. The dispersion may not have to be anomalous everywhere, and part of the low-dispersion band can have normal dispersion. In this way, the overall dispersion is lowered. Ideally, one can use a dispersion flattening technique [20,21] to achieve a dispersion curve with a small and constant β_2, but it is very challenging in practice due to device fabrication imperfections. Therefore, using the hybrid dispersion profile would be more realistic to lower the overall dispersion.

We consider a Si_3N_4 microring cavity as an example to show the robustness of cavity soliton formation with four ZDWs and the hybrid-dispersion-assisted pump power reduction. Figure 1 shows that a thin SiO_2 slot of 156 nm is inserted into a Si_3N_4 waveguide for dispersion flattening [6]. The two Si_3N_4 layers are 920 and 480 nm thick, respectively. The waveguide is 1300 nm wide. A resonator is formed by curving the waveguide with a radius of about 114 μm and a gap of 450 nm between the cavity and a bus waveguide for light coupling.

The flattened dispersion curve is obtained as shown in Fig. 2 (labeled as Slot WG1), which contains all-order dispersion (AOD). In Fig. 2, by changing the top Si_3N_4 thickness from 480 nm to 490, 495 and 500 nm (from WG1 to WG4), the overall dispersion can be lower. At the same time, four ZDWs appear in WG3 and WG4. The mode profiles at four frequencies for WG 1 are shown in the insets in Fig. 2. In fact, since octave-spanning combs are aimed, one has to consider frequency dependencies of all other parameters in modeling comb generation to ensure the accuracy, including frequency-dependent nonlinear coefficient associated with Kerr self-steepening (KSS), and spectrally varying coupling and loss that cause frequency-dependent Q-factor (FDQ) of the cavity, as shown in Fig. 3. The coupling coefficient and round-trip loss are calculated numerically by finite difference time-domain (FDTD) and finite-element method (FEM) separately. The cavity Q factor is calculated accordingly. Stimulated Raman scattering (SRS) and dispersive wave generation (DWG) are also important. A generalized nonlinear model is given in Ref. [25] to describe the responses of a cavity soliton to the above effects.

Cavity soliton formation is viewed as a result of balanced self-phase modulation and anomalous dispersion, and thus, FDQ, KSS, SRS, and DWG are all the perturbations to a cavity soliton. With them, although a cavity soliton can still be formed, one may have to increase pump power to stabilize the soliton. For example, in Fig. 4, we show the soliton pulsewidth as a function of pump power in a cavity formed using WG1, with a continuous-wave (CW) pump originally set at

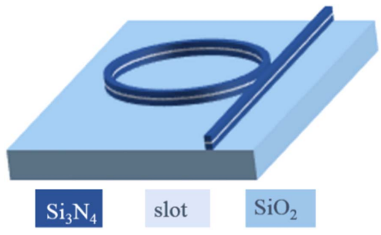

Fig. 1. Silicon nitride microring cavity produces hybrid dispersion by a nano-scale silica slot.

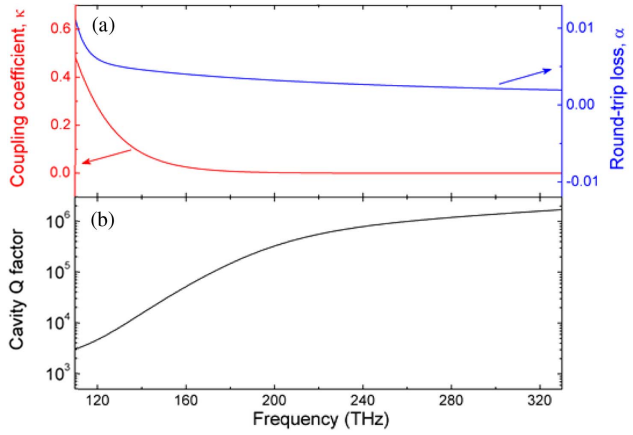

Fig. 3. Frequency dependences of the coupling coefficient, round-trip loss, and loaded Q-factor are shown in (a) and (b).

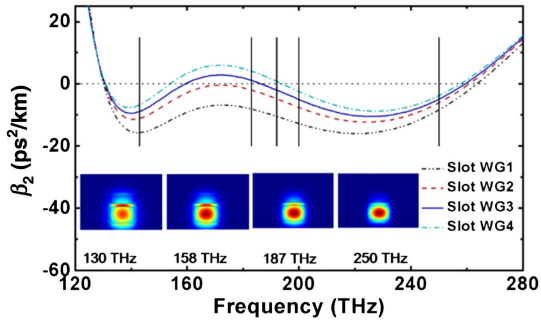

Fig. 2. By increasing the thickness of the top Si_3N_4 layer, the dispersion profile is tailored, with more normal dispersion occurring within the low-dispersion band. The vertical lines indicate pump locations for Fig. 6.

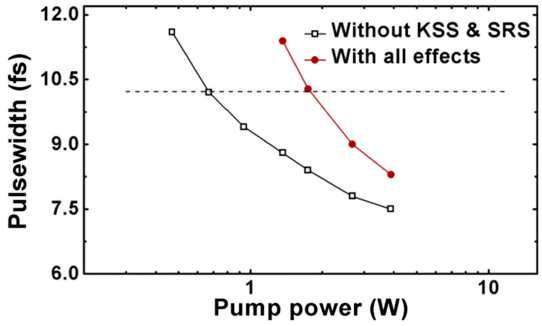

Fig. 4. Existence of KSS and SRS increases cavity soliton pulsewidth, and a higher pump power is required to obtain the same pulsewidth.

1500 nm. The results with all the above effects are compared with those obtained when KSS and SRS effects are ignored. Two-cycle (10 fs) cavity solitons can be obtained when the pump power is increased from 0.67 W to 1.74 W, with KSS and SRS taken into account (shown in the dashed line in Fig. 4). This power level is very challenging for an on-chip system. It is highly important to develop an effective way to reduce pump power for Kerr comb generation.

In a cavity, we find that such a hybrid dispersion profile can support a soliton. Kerr comb generation is simulated under different dispersion profiles in Fig. 2. Note that at first, we consider only the AOD effect in our model and ignore all other soliton effects, i.e., FDQ, DWG, KSS, and SRS. Intriguingly, a stable cavity soliton can be obtained in all the cases (WG1-WG4) with a pump at 1500 nm, which is in the anomalous region in all the dispersion profiles. It shows the great robustness of a soliton in the cavity in contrast to the case in the waveguide. We check the pump power versus pulsewidth shown in Fig. 5(a). The soliton pulsewidth can be kept at 7 fs as

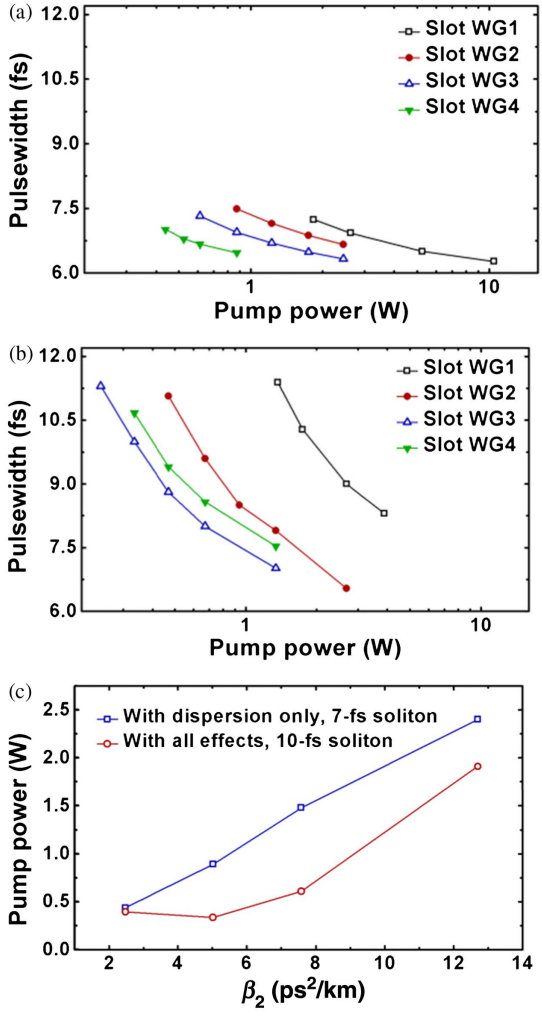

Fig. 5. Cavity soliton pulsewidth varies with pump power for different dispersion profiles that have increasingly more normal dispersion from WG1 to WG4 with (a) AOD only and (b) all perturbations. (c) Required pump power to produce a certain cavity soliton pulsewidth depends on the second-order dispersion value.

the required pump power decreases from 2.62 W to 0.49 W with more normal dispersion occurring from WG1 to WG4, because the overall dispersion is lower, when more normal dispersion is involved. When the top layer thickness is >500 nm, the overall dispersion becomes normal, and no cavity soliton is excited.

Then, we take all the soliton effects into account for a comparison. Similarly, cavity solitons can be obtained in all the dispersion curves. In Fig. 5(b), we also show the pump power versus pulsewidth. The pulsewidth becomes larger now, compared to the case with AOD only, with the same pump power. For a pulsewidth of 10 fs, the required pump power is reduced from 1.74 W to 0.34 W, as the dispersion profile is changed from WG1 to WG4. The above results show a very effective way to reduce pump power by using hybrid dispersion.

In Fig. 5(c), in the case with AOD only, we plot the required pump power to obtain a cavity soliton of 7 fs, and it decreases almost linearly with the second-order dispersion value by a factor of 6. In contrast, with all the perturbations turned on, the required power decreases first by a factor of 5 and becomes saturated then. The lowest required pump power does not occur at the smallest dispersion value. This can be explained by the following. To support a stable cavity soliton, we need self-phase modulation and a certain amount of anomalous dispersion. Without the soliton perturbation effects, such as FDQ, KSS, SRS, and DWG, the required dispersion is small, so the soliton energy associated with the pump power is also small. However, with the perturbations, a larger dispersion is needed to suppress the impact of the perturbations (otherwise, some of them, such as KSS, can be enhanced [25]) and to maintain the soliton. The smallest anomalous dispersion is not the best case anymore.

We further explore the wavelength flexibility for a cavity formed with WG3 or WG4, with hybrid dispersion profiles shown in Fig. 2. WG4 has more normal dispersion than WG3, and its overall anomalous dispersion is smaller. The pump is placed at different locations from 250 THz to 143 THz, covering the hybrid dispersion region for both waveguides, as labeled in Fig. 2. The normalized pump power X (defined in Ref. [24]) is kept the same, and accordingly the pump power is increased from 0.38 W to 1.2 W due to Q-factor degradation. As the pump frequency is scanned from 250 THz to 200 THz, mainly in the anomalous dispersion region for both waveguides, the generated combs can be mode locked, and the associated temporal profiles are shown in Figs. 6(a) and 6(b). However, as the pump is moved to 193 THz, which is already in the normal dispersion region for WG4, the combs would not be mode locked anymore, stopped at modulational instability stage finally, shown in Fig. 6(b), while solitons can still be formed for WG3, with the pump in the anomalous dispersion region. Note that when the pump is at 183 THz, i.e., further into the normal dispersion region for slot WG4, a mode-locked comb occurs again, but the formed pulse is distorted, showing several spikes in its waveform in Fig. 6(b). Accordingly, the spectrum spans over the normal dispersion region and extends to the anomalous dispersion regions on both sides. The spectrum is reshaped due to hybrid dispersion, and correspondingly the pulse is modulated. This effect vanishes, as the pump is further

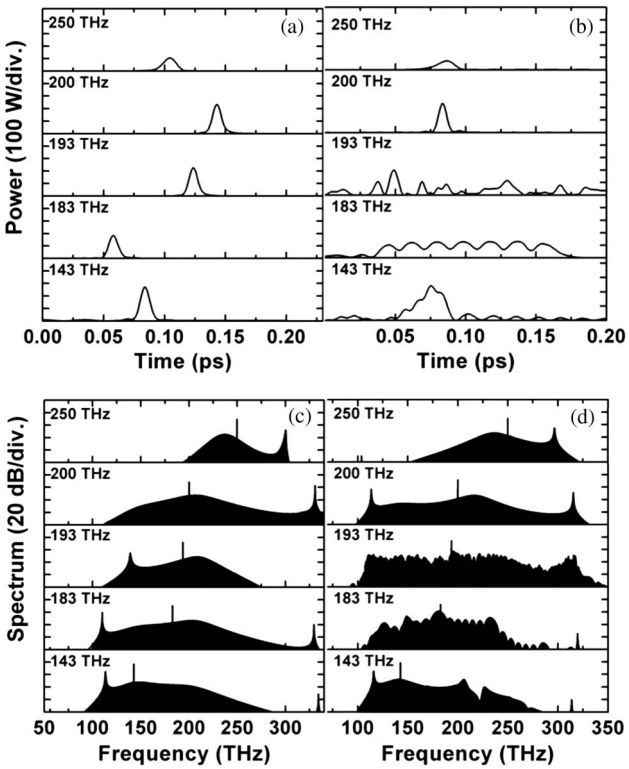

Fig. 6. Intra-cavity temporal waveforms with the pump placed at different wavelengths, as shown in Fig. 2, in a cavity formed with (a) WG3 and (b) WG4. The associated spectra are shown in (c) and (d).

scanned from 170 THz to 158 THz deep into the normal dispersion region for WG4, in which no new comb lines are generated (the corresponding waveforms are not shown in Fig. 6). With the pump placed here, the overall dispersion experienced by a comb will be normal, and thus no comb occurs. The pump over this band for WG3 is in the normal dispersion, too. However, the solitons are mode locked and have no temporal distortion due to a small fraction of the normal dispersion across the bandwidth. This shows the great robustness of cavity solitons. As the pump is moved to 143 THz, which is in the anomalous region again for both waveguides, mode-locking combs are formed again. The pulse is also slightly reshaped for WG4. Sometimes an intensity dip occurs in the pulse waveform, when we repeat the simulations for WG4 at 143 THz, as can be seen in Refs. [17,18]. The spectra for WG3 and WG4 are shown in Figs. 6(c) and 6(d). Note that at 183 THz for WG4, the spectrum has many oscillations and is not smooth any more. However, we check the average intra-cavity power as the pump is detuned and find that the power becomes constant after the detuning is stopped, indicating that the soliton is stable in the cavity.

3. SUMMARY

We have explored Kerr comb generation with a dispersion profile exhibiting four ZDWs. This study deepens our understanding of cavity soliton robustness with unique dispersion properties. More importantly, it opens a door to greatly reduce the pump power requirement for octave-spanning comb generation, with the pump power reduced by five to six times for the same comb bandwidth, which facilitates the realization of fully integrated octave-spanning combs. Wavelength flexibility is also explored, which shows the robustness of cavity solitons with such a hybrid dispersion profile.

Funding. National Basic Research Program of China (973) (2014CB340104/3); National Natural Science Foundation of China (NSFC) (61775164, 61335005, 61575142, 61431009); Advanced Integrated Optoelectronics Facility at the Tianjin University, China.

REFERENCES

1. P. Del'Haye, A. Schliesser, O. Arcizet, T. Wilken, R. Holzwarth, and T. J. Kippenberg, "Optical frequency comb generation from a monolithic microresonator," Nature **450**, 1214–1217 (2007).
2. J. S. Levy, A. Gondarenko, M. A. Foster, A. C. Turner-Foster, A. L. Gaeta, and M. Lipson, "CMOS-compatible multiple-wavelength oscillator for on-chip optical interconnects," Nat. Photonics **4**, 37–40 (2010).
3. Y. K. Chembo and N. Yu, "On the generation of octave-spanning optical frequency combs using monolithic whispering-gallery-mode microresonators," Opt. Lett. **35**, 2696–2698 (2010).
4. T. Herr, V. Brash, J. D. Jost, C. Y. Yang, N. M. Kondratiev, M. L. Gorodetsky, and T. J. Kippenberg, "Temporal solitons in optical microresonators," Nat. Photonics **8**, 145–152 (2014).
5. S.-W. Huang, H. Zhou, J. Yang, J. F. McMillan, M. Yu, D. L. Kwong, L. Maleki, and C. W. Wong, "Mode-locked ultrashort pulse generation from on-chip normal dispersion microresonators," Phys. Rev. Lett. **114**, 053901 (2015).
6. L. Zhang, C. Bao, V. Singh, J. Mu, C. Yang, A. M. Agarwal, L. C. Kimerling, and J. Michel, "Generation of two-cycle pulses and octave-spanning frequency combs in a dispersion-flattened microresonator," Opt. Lett. **38**, 5122–5125 (2013).
7. I. S. Grudinin, V. Huet, N. Yu, A. B. Matsko, M. L. Gorodetsky, and L. Maleki, "High-contrast Kerr frequency combs," Optica **4**, 434–437 (2017).
8. A. E. Dorche, S. Abdollahramezani, H. Taheri, A. A. Eftekhar, and A. Adibi, "Extending chip-based Kerr-comb to visible spectrum by dispersive wave engineering," Opt. Express **25**, 22362–22374 (2017).
9. C. Godey, I. V. Balakireva, A. Coillet, and Y. K. Chembo, "Stability analysis of the spatiotemporal Lugiato-Lefever model for Kerr optical frequency combs in the anomalous and normal dispersion regimes," Phys. Rev. A **89**, 722–729 (2014).
10. X. Xue, Y. Xuan, Y. Liu, P.-H. Wang, S. Chen, J. Wang, D. E. Leaird, M. Qi, and A. W. Weiner, "Mode-locked dark pulse Kerr combs in normal-dispersion microresonators," Nat. Photonics **9**, 594–600 (2015).
11. J. Wang, Y. Guo, H. Liu, G. Li, and L. Zhang, "A comparative analysis on fully integrated spectral broadening of Kerr frequency combs," IEEE Photon. J. **9**, 4502509 (2017).
12. G. P. Agrawal, *Nonlinear Fiber Optics*, 5th ed. (Academic, 2013).
13. P. Parrarivas, D. Gomilam, F. Leo, S. Coen, and L. Gelens, "Third-order chromatic dispersion stabilizes Kerr frequency combs," Opt. Lett. **39**, 2971–2974 (2014).
14. C. Millian and D. V. Skryabin, "Soliton families and resonant radiation in a micror-ring resonator near zero group-velocity dispersion," Opt. Express **22**, 3732–3749 (2014).
15. H. Taheri, A. B. Matsko, and L. Maleki, "Optical lattice trap for Kerr solitons," Eur. Phys. J. D **71**, 153 (2017).
16. D. C. Cole, E. S. Lamb, P. Del'Haye, S. A. Diddams, and S. B. Papp, "Soliton crystals in Kerr resonators," Nat. Photonics **11**, 671–676 (2017).
17. C. Bao, H. Taheri, L. Zhang, A. Matsko, Y. Yan, P. Liao, L. Maleki, and A. E. Willner, "High-order dispersion in Kerr comb oscillators," J. Opt. Soc. Am. B **34**, 715–725 (2017).

18. H. Taheri, "Ultrashort pulses in optical microresonators with Kerr nonlinearity," Ph.D. dissertation (Georgia Institute of Technology, 2017), Chap. 6.
19. J. Wang, Z. Han, Y. Guo, L. C. Kimerling, J. Michel, A. M. Agrarwal, G. Li, and L. Zhang, "Robust generation of frequency combs in a microresonator with strong and narrowband loss," Photon. Res. **5**, 552–556 (2017).
20. L. Zhang, Q. Lin, Y. Yue, Y. Yan, R. G. Beausoleil, and A. E. Willner, "Silicon waveguide with four zero-dispersion wavelengths and its application in on-chip octave-spanning supercontinuum generation," Opt. Express **20**, 1685–1690 (2012).
21. Y. Guo, Z. Jarari, A. M. Agarwal, L. C. Kimerling, G. Li, J. Michel, and L. Zhang, "Bilayer dispersion-flattened waveguides with four zero-dispersion wavelengths," Opt. Lett. **41**, 4939–4942 (2016).
22. P. Del'Haye, T. Herr, E. Gavartin, M. L. Gorodetsky, R. Holzwarth, and T. J. Kippenberg, "Octave spanning tunable frequency comb from a microresonator," Phys. Rev. Lett. **107**, 063901 (2011).
23. Y. Okawachi, K. Saha, J. S. Levy, Y. H. Wen, M. Lipson, and A. L. Gaeta, "Octave-spanning frequency comb generation in a silicon nitride chip," Opt. Lett. **36**, 3398–3400 (2011).
24. S. Coen and M. Erkintalo, "Universal scaling laws of Kerr frequency combs," Opt. Lett. **38**, 1790–1792 (2013).
25. L. Zhang, Q. Lin, L. C. Kimerling, and J. Michel, "Self-frequency shift of cavity soliton in Kerr frequency comb," arxiv: 14014.1137 (2014).